

# Thermal Diffusion and Diffusion Thermo Effects on the Motion of Viscoelastic Fluid through Porous Medium with Chemical Reaction under the Influence of Uniform Magnetic Field

Nabil T.M. El-dabe<sup>1</sup>, Mohammed Y. Abouzeid<sup>1,3</sup>, Hemat A. Sayed<sup>2</sup>

<sup>1</sup>Department of mathematics, Faculty of Education, Ain Shams University, Heliopolis, Cairo, Egypt  
Corresponding author's email: mastermath2003 {at} gmail.com

<sup>2</sup>Department of mathematics, Faculty of Science, Zagazig University, Egypt

<sup>3</sup>Department of mathematics, Faculty of Science, Tabuk University, Tabuk, KSA

---

**ABSTRACT---** *The motion of non-Newtonian fluid through porous medium inside the boundary layer of an infinite wall is considered. The fluid is obeying the viscoelastic type and the motion is under the effects of magnetic field with chemical reaction and heat generation. The problem is modulated mathematically by using the continuity, momentum, heat and mass transfer equations. The system of differential equations which describe this motion is solved numerically with appropriate boundary conditions by using finite difference scheme. Numerical results are presented to investigate the influence of the magnetic parameter, visco-elastic parameter, porous medium parameter, Prandtl number, heat source sink parameter, Dufour number, Hartmann number, Eckert number, Soret number, Schmidt number and the chemical reaction parameter on the stream function, temperature and concentration profiles. Several graphs for these results of physical interest are displayed and discussed in detail.*

**Keywords---** Viscoelastic Fluid ; Magnetic Field; Porous Medium; Thermal Diffusion; Diffusion Thermo; Chemical Reaction.

---

## 1- INTRODUCTION

The study of visco-elastic fluids has gained great importance in the last few years . Viscoelastic flows arise in numerous processes in chemical engineering system. Such flows possess both viscous and elastic properties. Veena et al. [1] investigated the study of non-similar solutions for an electrically conducting viscoelastic fluid flow with heat and mass transfer over a stretching sheet embedded in saturated porous medium. Eldabe and Sallam [2] studied the steady flow of an electrically conducting viscoelastic fluid in a saturated porous medium between two porous parallel plates with one plate moving and the other stationary. Also, they [3] considered the problem of the flow and heat transfer in the non-Newtonian viscoelastic electrically conducting incompressible fluid confined between two parallel plates one of them is a stretching plate and the other is a stationary porous plate through which there is a uniform injection. The effects of chemical reaction and heat radiation on the MHD flow of viscoelastic fluid through a porous medium over a horizontal stretching flat plate is studied by Eldabe et al. [4] . Alharbi et al [5] investigated the problem of convective heat and mass transfer of incompressible MHD viscoelastic fluid embedded in a porous medium over a stretching sheet under a chemical reaction. The effect of thermal diffusion of unsteady flow of a viscoelastic fluid through porous medium with heat source is investigated by Kumar et al. [6] in presence of a uniform magnetic field. Hayat et al .[7] discussed the characteristics of hydrodynamic flow and heat transfer analysis in a rotating frame of reference. An analysis was carried out by Abel and Joshi [8] to study the effect of heat transfer in MHD viscoelastic fluid over a non- isothermal stretching sheet with internal heat generation.

The heat and mass transfer simultaneously affecting each other that will cause the cross diffusion effect. The heat transfer caused by concentration gradient is called the diffusion- thermo or Dufour effect. On the other hand mass transfer caused by temperature gradient is called Soret or thermo-diffusion effect. Alam and Rahman [10] investigated Dufour and Soret effects on mixed convection flow past a vertical porous flat plate with variable suction. El-Arabawy [11] investigated the heat and mass transfer by natural convection from vertical surface embedded in a fluid-saturated porous

media considering Soret and Dufour effects with variable surface temperature and constant concentration. The thermal-diffusion and diffusion-thermo effects on mixed free-forced convection and mass transfer boundary layer flow of non-Newtonian fluid with temperature dependent viscosity are studied by Eldabe et al [12]. Also, Eldabe and Abu Zeid [13] investigated thermal diffusion and diffusion thermo effects on the viscous fluid flow with heat and mass transfer through porous medium over a shrinking sheet. The problem of non-Newtonian magnetohydrodynamic flow over a stretching surface with heat and mass transfer was studied by Abel et al [14].

The main aim of this work is to extend the work of Abel et al [14] to include the motion through porous medium in the presence of chemical reaction and considering thermal diffusion and diffusion thermo effects with Joule dissipations and viscous. The governing non-linear partial differential equations are transformed by using similarity transform into non-linear ordinary differential equations. The system of these equations with an appropriate boundary conditions are solved numerically by using the finite different method. The effects of various governing parameter on the stream function, temperature and concentration are shown in figures and discussed in details.

## NOMENCLATURE

$A_0, A_1$  constants

$B_0$  Strength of the magnetic field

$C$  Species concentration in the fluid

$c_p$  Specific heat at constant pressure

$C_\infty$  Ambient concentration of the fluid

$C_w$  The wall concentration of fluid

$D$  Mass diffusion coefficient

$Df$  Dufour number =  $\frac{D_m k_T (C_\sigma - C_\infty)}{v c_s c_p (T_\sigma - T_\infty)}$

$Ec$  Eckert number =  $\frac{\lambda^2 l^2}{A_0 c_p}$

$K$  The permeability parameter =  $\frac{\mu}{\rho k_p \lambda}$

$K_1$  The elasticity parameter =  $\frac{k_0 \lambda}{v}$

$L$  The chemical reaction parameter =  $\frac{k}{\lambda}$

$l$  The characteristic length

$M$  The magnetic parameter =  $\frac{\sigma B_0^2}{\lambda \rho}$

$Pr$  prandtl number =  $\frac{\mu c_p}{\alpha}$

$p$  The pressure

$Sc$  Shmidt number =  $\frac{v}{D_m}$

$Sr$  Sort number =  $\frac{D_m k_T (T_\sigma - T_\infty)}{v T_m (C_\sigma - C_\infty)}$

$t$  The transpose

$Ha$  Hartmann number =  $\sqrt{\frac{\sigma}{\rho}} B_0$

$T$  temperature of the fluid

$T_\infty$  Ambient temperature of the fluid

$T_w$  wall temperature of the fluid

$v$  transverse velocity in thy directions

Greek symbol

$\alpha$  Coefficient of thermal conductivity

$\alpha_1, \alpha_2$  are the normal stress modulus

$\beta = \frac{Q}{\rho \lambda c_p}$  The heat source sink

$\rho$  Density of fluid, electrical

$\lambda$  Constant

$\mu$  The coefficient of viscosity

$\nu$  The kinematic of viscosity

$\sigma^*$  Stefan- Boltzman constant parameter

$\tau$  The stress tensor

$\tau_{xy}$  Component of the stress tensor

## 2- FLOW ANALYSIS

Consider the two- dimensional laminar boundary layer flow of an incompressible viscoelastic fluid through porous medium with heat and mass transfer past an infinite plate.

The system is stressed by the influence of magnetic field in the presence of chemical reaction and heat generation. Choose the Cartesian coordinates  $(x, y)$  where  $x$  - axis is along the infinite plate while  $y$  - axis is perpendicular to it. The constitutive equation of the viscoelastic fluid which illustrates the relation between stress and rate of strain can be written as

$$\tau = -pI + \mu A_1 + \alpha_1 A_2 + \alpha_2 A_1^2 \quad (1)$$

Here  $A_1$  and  $A_2$  are defined as

$$A_1 = (\text{grad } v) + (\text{grad } v)^t \quad (2)$$

$$A_2 = \left(\frac{d}{dt} A_1\right) + A_1 \cdot (\text{grad } v) + (\text{grad } v)^t \cdot A_1 \quad (3)$$

The thermodynamics and stability of the model in Eq. (1) were studied in detail by Dunn and Fosdick [9]. Thermodynamics compatibility in the sense that all motions of the fluid meet the Clausius-Duhem inequality (generally interpreted as a statement of the second law of thermodynamics) and the assumption that the specific Helmholtz free energy of the fluid be a minimum when the fluid is locally at rest requires that

$$\mu \geq 0, \quad \alpha_1 \geq 0, \quad \alpha_1 + \alpha_2 = 0 \quad (4)$$

In our analysis we assume that the fluid is thermodynamically compatible; hence the stress constitutive relation, Eq. (1) reduces to

$$\tau = -pI + \mu A_1 + \alpha_1 A_2 - \alpha_1 A_1^2 \quad (5)$$

## 3-GOVERNING EQUATIONS

In Cartesian coordinates the continuity, momentum, temperature and concentration equations can be written as  
The continuity equation

$$\frac{\partial u}{\partial x} + \frac{\partial v}{\partial y} = 0 \quad (6)$$

The momentum equation

$$u \frac{\partial u}{\partial x} + v \frac{\partial u}{\partial y} = \nu \frac{\partial^2 u}{\partial y^2} - \left(\frac{\mu}{\rho k_p} + \frac{\sigma B_0^2}{\rho}\right) u - \frac{k_0}{\rho} \left\{ \frac{\partial}{\partial x} \left( u \frac{\partial^2 u}{\partial y^2} \right) + \frac{\partial u}{\partial y} \frac{\partial^2 v}{\partial y^2} + v \frac{\partial^3 u}{\partial y^3} \right\} \quad (7)$$

The energy equation (heat transfer) is

$$u \frac{\partial T}{\partial x} + v \frac{\partial T}{\partial y} = \frac{\alpha}{\rho c_p} \frac{\partial^2 T}{\partial y^2} + \frac{\sigma B_0^2}{\rho c_p} u^2 - k_0 \frac{\partial u}{\partial y} \left\{ \frac{\partial}{\partial y} \left( u \frac{\partial u}{\partial x} + v \frac{\partial u}{\partial y} \right) \right\} + \frac{D_m k_T}{c_s c_p} \frac{\partial^2 C}{\partial y^2} + Q(T - T_\infty) \quad (8)$$

The diffusion equation ( mass transfer) is

$$u \frac{\partial C}{\partial x} + v \frac{\partial C}{\partial y} = D_m \frac{\partial^2 C}{\partial y^2} + k_1 C + \frac{D_m k_T}{T_m} \frac{\partial^2 T}{\partial y^2} \quad (9)$$

The appropriate boundary conditions governing the problem are :

$$\left. \begin{aligned} u = u_w = c x, \quad v = 0, \quad T = T_w = T_\infty + A_0 \left(\frac{x}{l}\right)^2, \quad C = C_w = C_\infty + A_1 \left(\frac{x}{l}\right) \quad \text{at } y = 0 \\ u \rightarrow 0, \quad v \rightarrow 0, \quad T \rightarrow T_\infty, \quad C \rightarrow C_\infty \quad \text{as } y \rightarrow \infty \end{aligned} \right\} \quad (10)$$

The equation of continuity is satisfied if we choose a dimensionless stream function  $\psi$  such that

$$u = \frac{\partial \psi}{\partial y} \text{ and } v = -\frac{\partial \psi}{\partial x} \quad (11)$$

Introducing the similarity transformations

$$\eta = \sqrt{\frac{\lambda}{\nu}} y \quad f(\eta) = -\frac{\psi(x, y)}{x\sqrt{\nu\lambda}} \quad (12)$$

Using Eqs. (11) and (12), the velocity components become

$$u = \lambda x f'(\eta), \quad v = -\sqrt{\nu\lambda} f(\eta) \quad \text{and also } \theta = \frac{T - T_\infty}{T_w - T_\infty}, \quad \phi = \frac{C - C_\infty}{C_w - C_\infty}, \quad \psi = \frac{\mu}{\rho}. \quad (13)$$

Where a prime denotes differentiation with respect to  $\eta$ .

Substitution from Eq. (13) in Eqs. (7-9) we get

$$\left. \begin{aligned} f'^2 - f f'' &= f''' - (K + M)f' - K_1(2f' f''' - f''^2 - f f^{(4)}) \\ \text{Pr}(2f'\theta - \theta'f) &= \theta'' + \text{Ec Pr}(\text{Ha})^2 f'^2 + \text{Df Pr} \phi'' + \beta \text{Pr} \theta - K_1 \text{Ec}(f' f''^2 - f f'' f''') \\ (2f'\phi - f \phi')\text{Sc} &= \phi'' + \text{Sc}(\text{Sr} \theta'' + L \phi) \end{aligned} \right\} \quad (14)$$

subject to the following

$$\left. \begin{aligned} f' = 1, f = 0, \theta = 1, \phi = 1 & \quad \text{with } \eta \rightarrow 0 \\ f' = 0, f = 0, \theta = 0, \phi = 0 & \quad \text{as } \eta \rightarrow \infty \end{aligned} \right\} \quad (15)$$

The system of coupled equations (14), subjected to the boundary conditions (15), is solved numerically by using the finite difference scheme in the following section.

#### 4- NUMERICAL RESULTS AND DISCUSSION

The system of equations that govern the motion with heat and mass transfer of magnetohydrodynamic are solved numerically by using the explicit finite difference scheme. The numerical formulas for stream function, temperature and concentration are obtained as a functions of the physical parameters of the problem.

The effects of physical parameters on the stream function  $\psi$  are indicated through figures (1-3). Figures (1) and (2), illustrate the effects of the permeability parameter  $K$  and the elasticity  $K_1$  respectively. It is found that the stream function  $\psi$  increases with increasing  $K$ , but it decreases with increasing  $K_1$ . we also noted that the stream function  $\psi$  increases till a definite maximum value at  $\eta = \eta_0$  and it decreases afterwards. This maximum value of  $\psi$  increases by increasing  $K$  while it decreases by increasing  $K_1$ .

The effect of the magnetic parameter  $M$  on the stream function  $\psi$  is shown in figure (3), and it is shown that the stream function  $\psi$  increases by increasing  $M$ , and also noted that the stream function  $\psi$  increases till a definite maximum value at  $\eta = \eta_0$  and it decreases afterwards.

The temperature distribution  $\theta$  for different values of Eckert number  $\text{Ec}$  is obtained graphically through figure (4), we observed that the temperature distribution  $\theta$  decreases with the increasing of  $\text{Ec}$  in the region  $0 < \eta < 3$ . Afterwards  $\theta$  increases with increasing  $\text{Ec}$ , and the obtained curves intersect approximately at  $\eta = 3$ . It is also noted that  $\theta$  decreases with the increase of  $x$  till a definite value  $\eta = \eta_0$  (represents the minimum value of  $\theta$ ) and it increases afterwards till a maximum value of  $\theta$ , then it decreases again. In Figs. (5-8), the effects of the permeability  $K$ , the elasticity parameter  $K_1$ , the magnetic field  $M$  and Prandtl number  $\text{Pr}$  on the temperature distribution  $\theta$  respectively. In these figures, we observed that the effects both of  $K$ ,  $K_1$ ,  $M$  and  $\text{Pr}$  on  $\theta$  are similar to the effect of  $\text{Ec}$  on  $\theta$  with the only different that the obtained curves are very close to those obtained in Fig. (4).

The effect of Dufour number  $\text{Df}$  on the temperature distribution  $\theta$  is shown in figure (9), and it is shown that the temperature  $\theta$  increases by increasing of  $\text{Df}$ . The change of the temperature distribution  $\theta$  with for different values of the Schmidt number  $\text{Sc}$  shown through Fig. (10), it is clear that the temperature distribution increases by increasing of

Sc . Figs. (11) and (12) illustrate that the behaviors of the temperature distribution  $\theta$  with different values of the chemical reaction  $L$  and the Hartmann number  $Ha$  respectively. It is found that  $\theta$  increases with increasing  $L$ , while it decreases with increasing  $Ha$ . We noted that the curves coincide in the region  $0 < \eta < 1$ , afterwards increases by increasing  $L$  but decreases by decreasing of  $Ha$ . The temperature distribution  $\theta$  for different values of  $Sr$  is displayed in Fig. (13). The graphical results of fig. (13) indicate that the temperature  $\theta$  increases as  $Sr$  increases. It is obvious that the curves of  $\theta$  are coincide in the region  $0 < \eta < 2$  and afterwards the temperature  $\theta$  increases by increasing of  $Sr$ . In figure (14), the graphs of the temperature distribution  $\theta$  have been drawn for different values of the heat source sink  $\beta$ . It is seen that, the behavior of the curves are coincide in the region  $0 < \eta < 3$  and afterwards  $\theta$  decreases by increasing of  $\beta$ .

Figure (15) and (16), show that the behaviors of the concentration distribution  $C$  for different values of permeability parameter  $K$  and the elasticity parameter  $K_1$  respectively. It is found that the concentration  $C$  increases with increasing the porosity parameter  $K$ , whereas it decreases with increasing elasticity parameter  $K_1$ . We also noted that the curves are coincide in the region  $0 < \eta < 1$  and afterwards, the concentration  $C$  increases by increasing  $K$  and the concentration  $C$  decreases by increasing of  $K_1$ . The effects of Schmidt number  $Sc$  on the concentration distribution  $C$  is shown in figure (17), and it is shown that the concentration  $C$  increases by increasing  $Sc$ . It is observed also that the behavior of the curves are coincide in the region  $0 < \eta < 1$  and afterwards, the concentration  $C$  increases by increasing of  $Sc$ .

The effects of the magnetic field parameter  $M$  and the chemical reaction parameter  $L$  on the concentration distribution are shown in figures (18) and (19). It is seen the behavior of the curves are the same as that obtained in Fig. (17), except that the obtained curves are close to those obtained in Fig. (17).

Finally, Fig. (20), illustrates the changes of the concentration  $C$  with Soret number  $Sr$ . It is clear that the concentration  $C$  increases with increasing of  $Sr$ .

## 5- CONCLUSION

. This problem is modulated mathematically by a set of differential equations which described the motion of the viscoelastic fluid with heat and mass transfer. These equations are transformed into an ordinary differential equations by using a similarity method which are solved numerically by using explicit finite difference scheme with appropriate boundary conditions. The effects of the parameters of the problem on these solutions are discussed and observed through several figures. The very important points conclusion can be written :

- a. The stream function  $\psi$  increases with the increase in magnetic parameter  $M$  and porosity parameter  $K$  increases.
- b. The stream function  $\psi$  decreases when elasticity parameter  $K_1$  increase.
- c. The temperature  $\theta$  increases when the Prantl number  $Pr$ , Dufour number  $Df$ , the Schmidt number  $Sc$ , porosity parameter  $K$ , elasticity parameter  $K_1$ , the magnetic field parameter  $M$ , the chemical reaction parameter  $L$ , the Soret number  $Sr$  and the Eckert number  $Ec$  increase.
- d. The temperature decreases when the heat source sink  $\beta$  and the Hartmann number  $Ha$  decrease.
- e. The concentration  $C$  increases when the Schmidt number  $Sc$ , the porosity parameter  $K$ , the magnetic parameter  $M$ , the chemical reaction parameter  $L$ , and Soret number  $Sr$  increase.
- f. We noted that the concentration  $C$  and The stream function  $\psi$  decrease when the function  $\psi$  decrease when the elasticity parameter  $K_1$  increases.

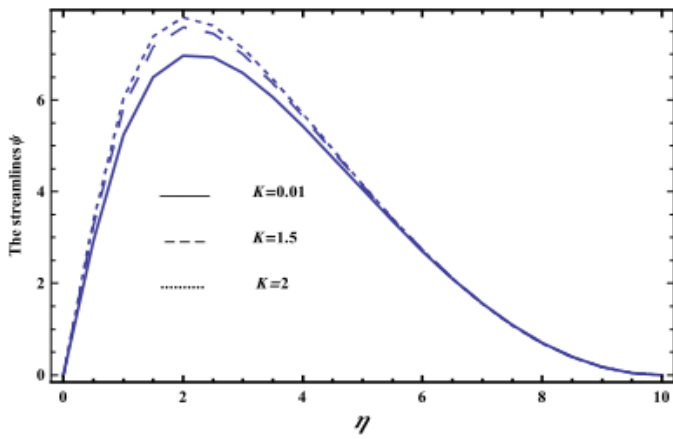


Figure (1)

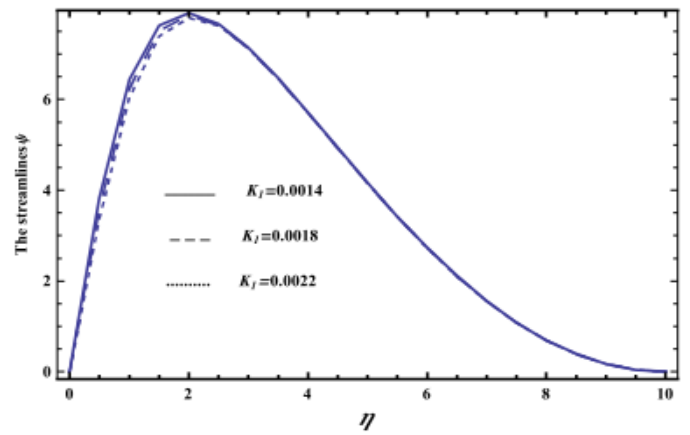


Figure (2)

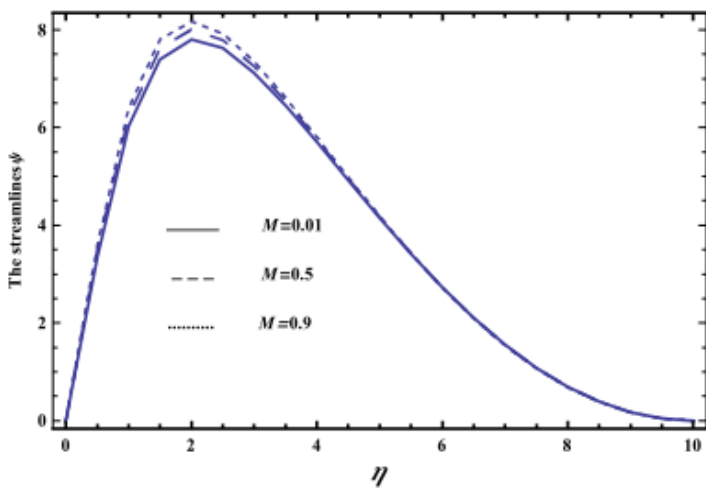


Figure (3)

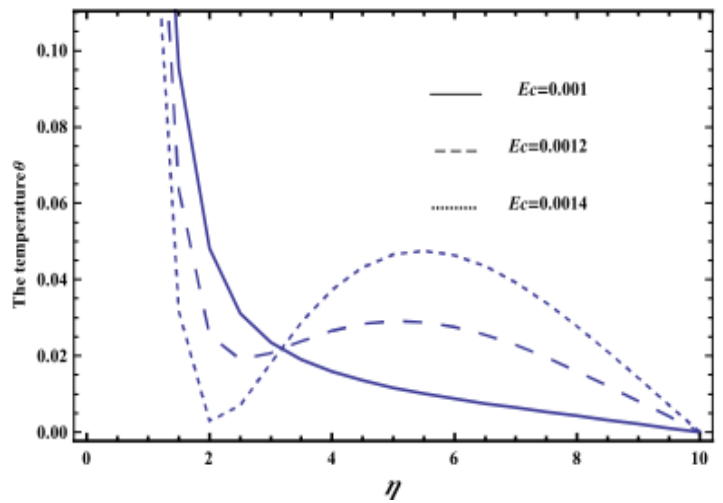
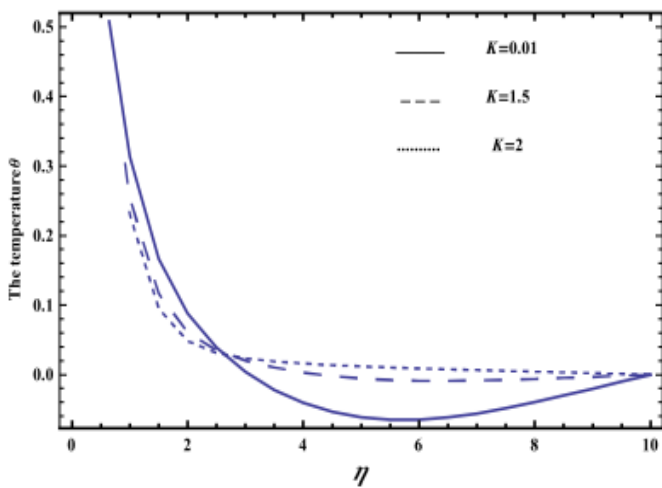
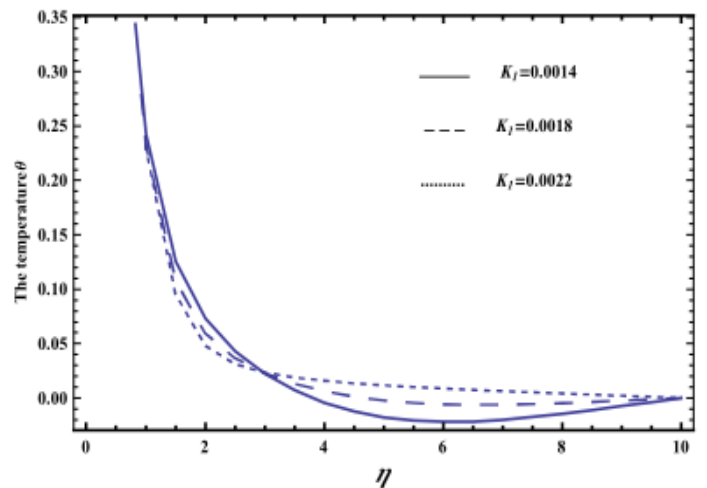


Figure (4)



Figure(5)



Figure(6)

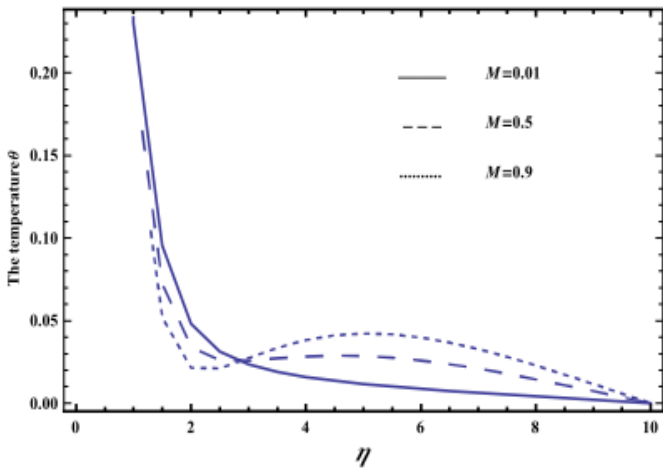


Figure (7)

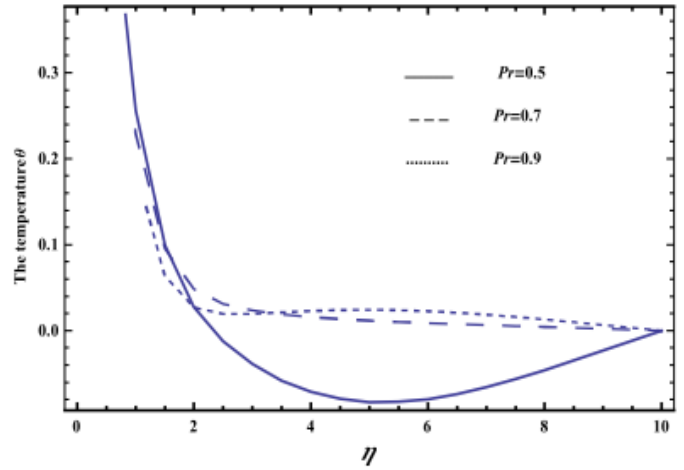


Figure (8)

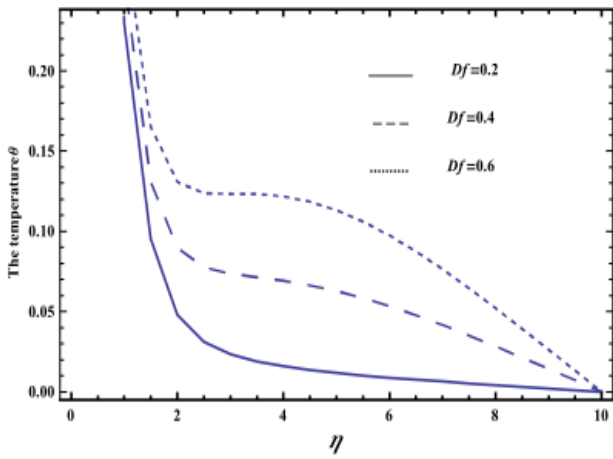


Figure (9)

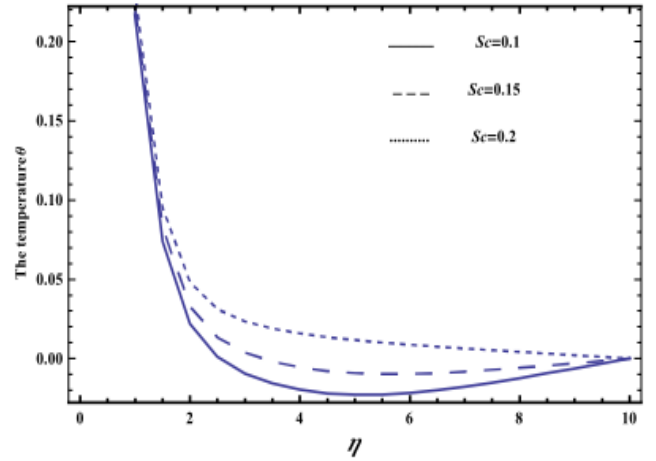


Figure (10)

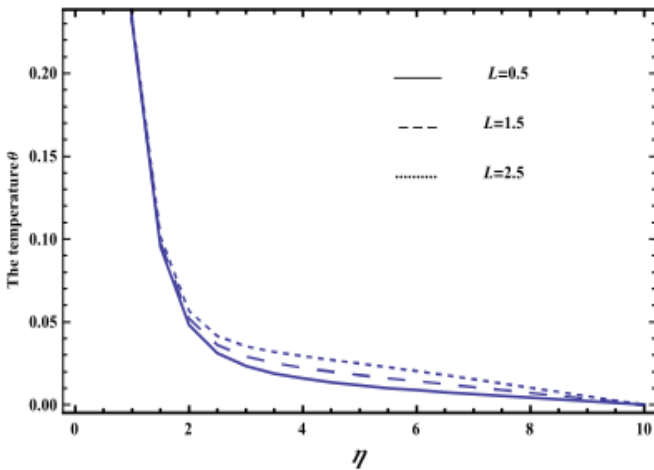


Figure (11)

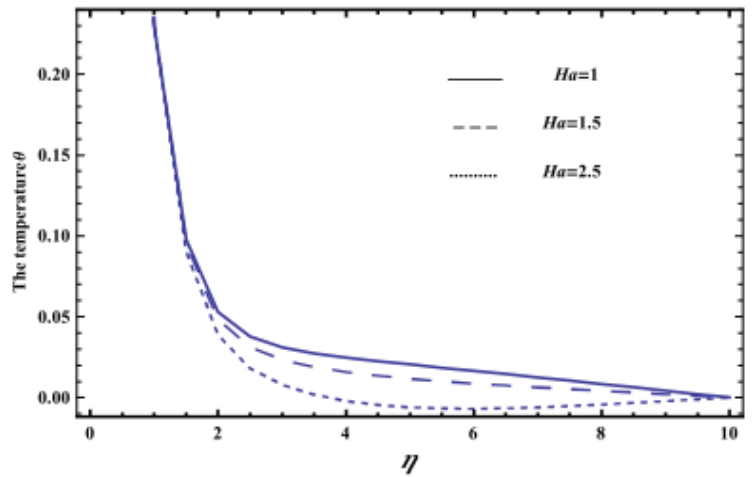
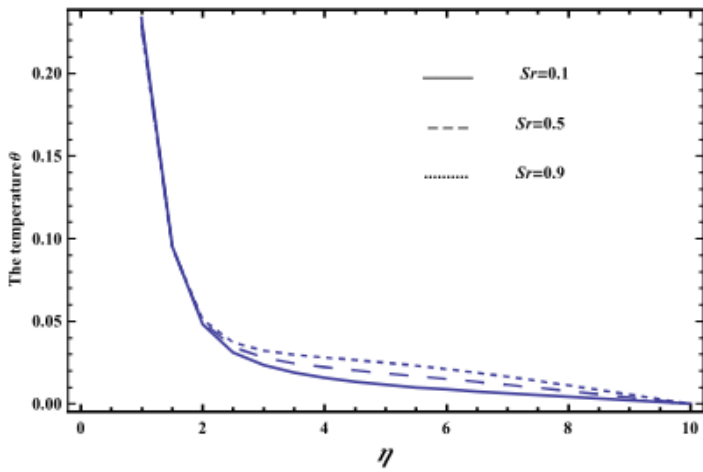


Figure (12)



Figure(13)

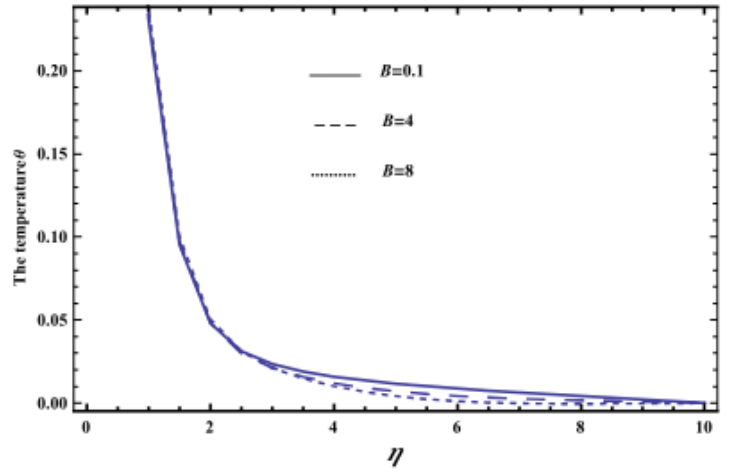


Figure (14)

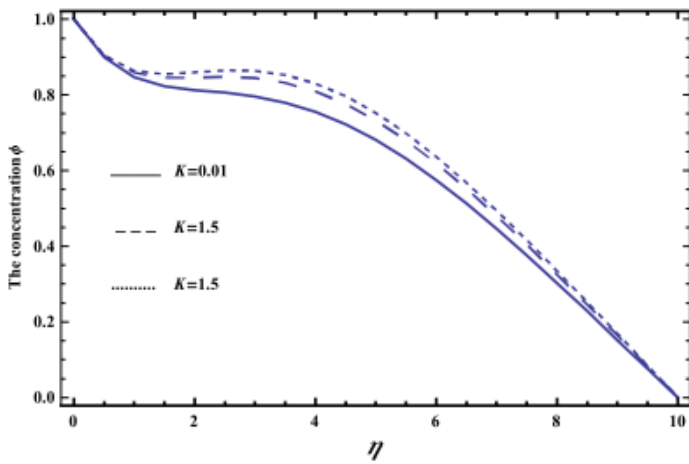


Figure (15)

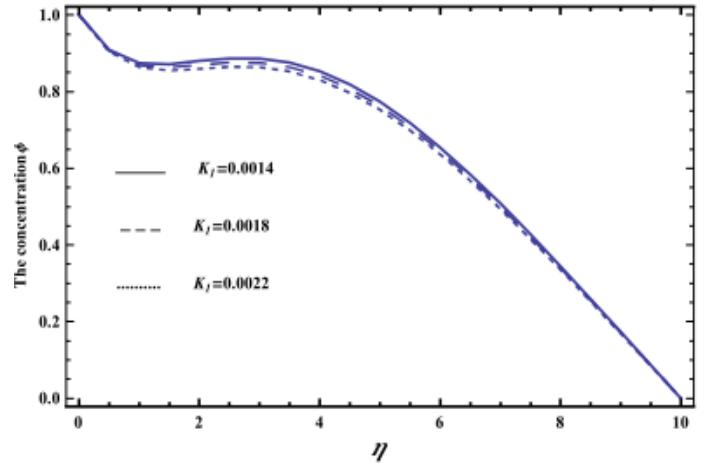


Figure (16)

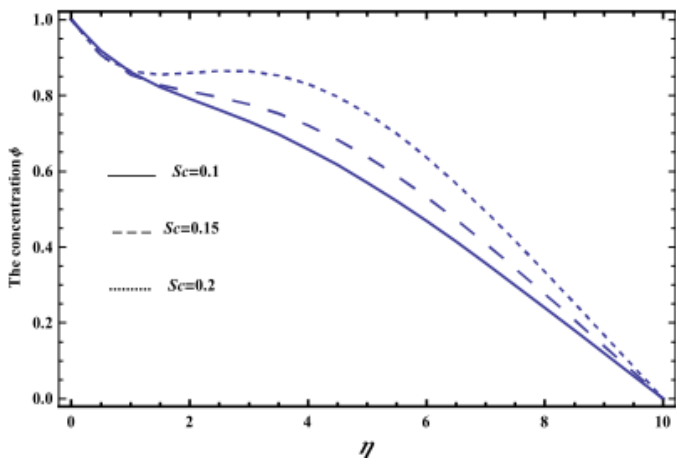


Figure (17)

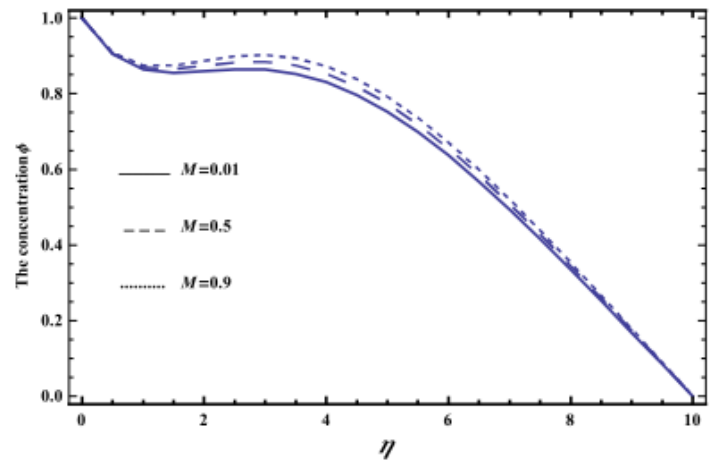


Figure (18)

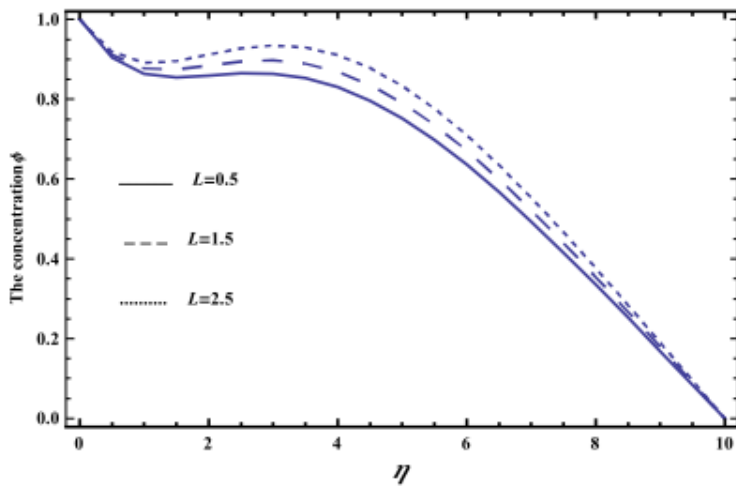


Figure (19)

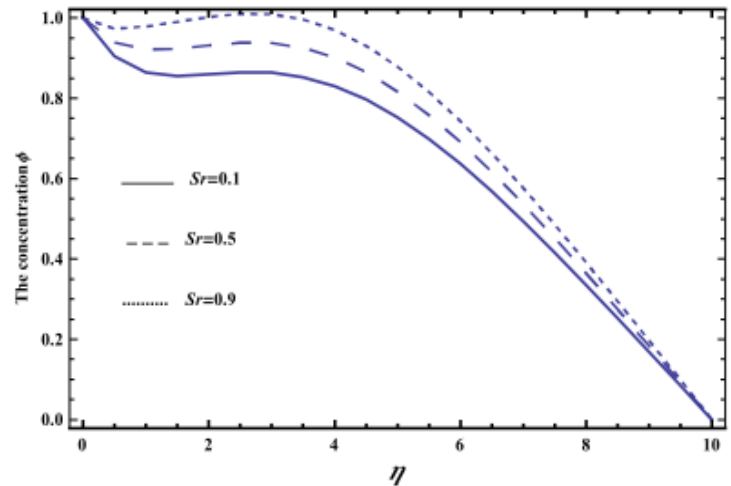


Figure (20)

## REFERENCES

- 1- P. H. Veena, V. K. Pravin, S. M. Shahjahan and V. B. Hippargi, "Non similar solution for heat and mass transfer flow in an electrically conducting viscoelastic fluid over a stretching sheet embedded in a porous medium", *Int. J. Modern Mathematics*, vol. 2(1), pp. 9-26, (2007).
- 2- N. T. El dabe and S. N. Sallam, "Non- Darcy couette flow through a porous medium of magnetohydrodynamic viscoelastic fluid with heat and mass transfer", *Can. J. Phys.*, vol. 83, pp. 1241-1263, (2005).
- 3- N. T. El dabe and S. N. Sallam, "MHD flow and heat transfer in a viscoelastic incompressible fluid confined between a horizontal stretching sheet and a parallel porous wall", *Can. J. Phys.*, vol. 76, pp. 949-964, (1998).
- 4- N. T. El dabe, A. G. Elsaka, A. E. Radwan and M. A. M. Eltaweel, "Effects of chemical reaction and heat radition on the MHD flow of viscoelastic fluid through a porous medium over a horizontal stretching flate plate", *J. American Science*, (2010).
- 5- S. M. Alharbi, V. K. Pravin, S. M. Shahjahan and V. B. Hippargi, "Non similar solution for heat and mass transfer flow in an electrically conducting viscoelastic fluid over a stretching sheet embedded in a porous medium", *Int. J. Modern Mathematics*, vol. 2(1), pp. 9-26, (2007).
- 6- V. Kumar, R. Johari and R. Jha, "Effect of thermal diffusion on MHD flow of a visco-elastic(Walter's liquid model-B) fluid through porous medium with heat source", *Int. J. Math. Res.*, vol. 6, pp. 599-606, (2011).
- 7- T. Hayat, Z. Abbas and S. Asghars. "Heat transfer analysis on rotation flow of a second grade fluid past a porous plate with variable suction". *Math. Prob.Eng* 5:5; pp.555-82, 2005.
- 8- S. Abel, M. Joshi and R. M. Sonth, "Heat transfer in MHD viscoelastic fluid over a stretching surface", *ZAMM* 81 (10),pp. 691-698, (2001).
- 9- J. E. Dunn, R. L. Fosdick, "Thermodynamics, stability, and boundedness of fluid of complexity 2 and fluids of second grade", *Arch. Rat.Mech. Anal.* 56,p.191, (1974).
- 10- M. S. Alam, and M. M. Rahman, "Dufour and Soret effects on mixed convection flow past a vertical porous flat plate with variable suction", *Nonlinear Anal Model Control*, vol. 11, pp. 3-12, (2006).
- 11- H. A. M. El-Arabawy, "Soret and Dufour effects on natural convection flow past a vertical in a porous medium with variable surface temperature", *J. Math. Stat.*, vol. 5(3), pp.190-198,(2009).

12- N. T. El dabe, A. G. El-Saka and A. Fouad, “Thermal-diffusion and diffusion-thermo effects on mixed free-forced convection and mass transfer boundary layer flow for non-Newtonian fluid with temperature dependent viscosity”. Applied Mathematics and Computation 152 (3):pp. 867-883, (2004).

13- N. T. El dabe and M. Abu Zeid: “Thermal diffusion and diffusion thermo effects on the viscous fluid flow with heat and mass transfer through porous medium over a shrinking sheet”. J. Applied Mathematics 2013.

14- S. Abel, P. H. Veena, K. Rajgopal and V. K. Pravin, “Non-Newtonian magneto-hydrodynamic flow over a stretching surface with heat and mass transfer”, International Journal of Non-Linear Mechanics 39, pp.1067-1078,(2004).

### FIGURE CAPTIONS

Fig. (1), the stream line  $\psi$  is plotted against  $\eta$ , for various values of the porous medium parameter  $K = 0.01, 1.5, 2$ , when  $M = 0.01, K_1 = 0.0022$ ,  $Pr = 0.7$ ,  $\beta = 0.1$ ,  $Df = 0.2$ ,  $Ha = 1.5$ ,  $Ec = 0.001$ ,  $Sr = 0.1$ ,  $Sc = 0.2$  and  $L = 0.5$ .

Fig. (2), the stream line  $\psi$  is plotted against  $\eta$ , for various values of the viscoelastic parameter  $K_1 = 0.0014, 0.0018, 0.0022$ , when  $M = 0.01, K = 2$ ,  $Pr = 0.7$ ,  $\beta = 0.1$ ,  $Df = 0.2$ ,  $Ha = 1.5$ ,  $Ec = 0.001$ ,  $Sr = 0.1$ ,  $Sc = 0.2$  and  $L = 0.5$ .

Fig. (3), the stream line  $\psi$  is plotted against  $\eta$ , for various values of the magnetic field parameter  $M = 0.01, 0.5, 0.9$ , when  $K = 2, K_1 = 0.0022$ ,  $Pr = 0.7$ ,  $\beta = 0.1$ ,  $Df = 0.2$ ,  $Ha = 1.5$ ,  $Ec = 0.001$ ,  $Sr = 0.1$ ,  $Sc = 0.2$  and  $L = 0.5$ .

Fig. (4), the temperature profile is plotted against  $\eta$ , for various values of the porous medium parameter  $K = 0.01, 1.5, 2$ , when  $M = 0.01, K_1 = 0.0022$ ,  $Pr = 0.7$ ,  $\beta = 0.1$ ,  $Df = 0.2$ ,  $Ha = 1.5$ ,  $Ec = 0.001$ ,  $Sr = 0.1$ ,  $Sc = 0.2$  and  $L = 0.5$ .

Fig. (5), the temperature profile is plotted against  $\eta$ , for various values of the viscoelastic parameter  $K_1 = 0.0014, 0.0018, 0.0022$ , when  $M = 0.01, K = 2$ ,  $Pr = 0.7$ ,  $\beta = 0.1$ ,  $Df = 0.2$ ,  $Ha = 1.5$ ,  $Ec = 0.001$ ,  $Sr = 0.1$ ,  $Sc = 0.2$  and  $L = 0.5$ .

Fig. (6), the temperature profile is plotted against  $\eta$ , for various values of the magnetic field parameter  $M = 0.01, 0.5, 0.9$  when  $K = 2, K_1 = 0.0022$ ,  $Pr = 0.7$ ,  $\beta = 0.1$ ,  $Df = 0.2$ ,  $Ha = 1.5$ ,  $Ec = 0.001$ ,  $Sr = 0.1$ ,  $Sc = 0.2$  and  $L = 0.5$ .

Fig. (7), the temperature profile is plotted against  $\eta$ , for various values of Eckert number  $Ec = 0.001, 0.0012, 0.0014$ , when  $M = 0.01, K_1 = 0.0022$ ,  $Pr = 0.7$ ,  $\beta = 0.1$ ,  $Df = 0.2$ ,  $Ha = 1.5$ ,  $K = 2$ ,  $Sr = 0.1$ ,  $Sc = 0.2$  and  $L = 0.5$ .

Fig. (8), the temperature profile is plotted against  $\eta$ , for various values of the Prandtl number  $Pr = 0.5, 0.7, 0.9$ , when  $M = 0.01, K_1 = 0.0022$ ,  $K = 2$ ,  $\beta = 0.1$ ,  $Df = 0.2$ ,  $Ha = 1.5$ ,  $Ec = 0.001$ ,  $Sr = 0.1$ ,  $Sc = 0.2$ ,  $L = 0.5$ .

Fig. (9), the temperature profile is plotted against  $\eta$ , for various values of the Dfour number  $Df = 0.2, 0.4, 0.6$ , when  $M = 0.01, K_1 = 0.0022$ ,  $Pr = 0.7$ ,  $\beta = 0.1$ ,  $K = 2$ ,  $Ha = 1.5$ ,  $Ec = 0.001$ ,  $Sr = 0.1$ ,  $Sc = 0.2$ .

and  $L = 0.5$ .

Fig. (10), the temperature profile is plotted against  $\eta$ , for various values of Schmidt number  $Sc = 0.1, 0.15, 0.2$ , when  $M = 0.01, K_1 = 0.0022$ ,  $Pr = 0.7$ ,  $\beta = 0.1$ ,  $Df = 0.2$ ,  $Ha = 1.5$ ,  $Ec = 0.001$ ,  $Sr = 0.1$ ,  $K = 2$  and  $L = 0.5$ .

Fig. (11), the temperature profile is plotted against  $\eta$ , for various values of the chemical reaction parameter  $L = 0.5, 1.5, 2.5$ , when  $M = 0.01, K_1 = 0.0022$ ,  $K = 2$ ,  $\beta = 0.1$ ,  $Df = 0.2$ ,  $Ha = 1.5$ ,  $Ec = 0.001$ ,  $Sr = 0.1$ ,  $Sc = 0.2$  and  $Pr = 0.7$ .

Fig. (12), the temperature profile is plotted against  $\eta$ , for various values of Hartmann number  $Ha = 1, 1.5, 2.5$ , when  $M = 0.01, K_1 = 0.0022$ ,  $Pr = 0.7$ ,  $\beta = 0.1$ ,  $Df = 0.2$ ,  $K = 2$ ,  $Ec = 0.001$ ,  $Sr = 0.1$ ,  $Sc = 0.2$  and  $L = 0.5$ .

Fig. (13), the temperature profile is plotted against  $\eta$ , for various values of the Soret number  $Sr = 0.1, 0.5, 0.9$ , when  $M = 0.01, K_1 = 0.0022$ ,  $Pr = 0.7$ ,  $\beta = 0.1$ ,  $Df = 0.2$ ,  $K = 2$ ,  $Ec = 0.001$ ,  $Ha = 1.5$ ,  $Sc = 0.2$  and  $L = 0.5$ .

Fig. (14), the temperature profile is plotted against  $\eta$ , for various values of heat source sink parameter  $\beta = 0.1, 4, 8$ , when  $M = 0.01, K_1 = 0.0022$ ,  $Pr = 0.7$ ,  $K = 2$ ,  $Df = 0.2$ ,  $Ha = 1.5$ ,  $Ec = 0.001$ ,  $Sr = 0.1$ ,  $Sc = 0.2$  and  $L = 0.5$ .

Fig. (15), the concentration profile is plotted against  $\eta$ , for various values of the porous medium parameter  $K = 0.01, 1.5, 2$ , when  $M = 0.01, K_1 = 0.0022$ ,  $Pr = 0.7$ ,  $\beta = 0.1$ ,  $Df = 0.2$ ,  $Ha = 1.5$ ,  $Ec = 0.001$ ,  $Sr = 0.1$ ,  $Sc = 0.2$  and  $L = 0.5$ .

Fig. (16), the concentration profile is plotted against  $\eta$ , for various values of the viscoelastic parameter  $K_1 = 0.0014, 0.0018, 0.0022$ , when  $M = 0.01, K_1 = 0.0022$ ,  $Pr = 0.7$ ,  $\beta = 0.1$ ,  $Df = 0.2$ ,  $Ha = 1.5$ ,  $Ec = 0.001$ ,  $Sr = 0.1$ ,  $Sc = 0.2$  and  $L = 0.5$ .

Fig. (17), the concentration profile is plotted against  $\eta$ , for various values of Schmidt number  $Sc = 0.2, 1, 1.5$ , when  $M = 0.01, K_1 = 0.0022$ ,  $Pr = 0.7$ ,  $\beta = 0.1$ ,  $Df = 0.2$ ,  $Ha = 1.5$ ,  $Ec = 0.001$ ,  $Sr = 0.1$ ,  $Sc = 0.2$  and  $L = 0.5$ .

Fig. (18), the concentration profile is plotted against  $\eta$ , for various values of the magnetic field parameter  $M = 0.01, 0.5, 0.9$  when  $K = 2, K_1 = 0.0022$ ,  $Pr = 0.7$ ,  $\beta = 0.1$ ,  $Df = 0.2$ ,  $Ha = 1.5$ ,  $Ec = 0.001$ ,  $Sr = 0.1$ ,  $Sc = 0.2$  and  $L = 0.5$ .

Fig. (19), the concentration profile is plotted against  $\eta$ , for various values of the chemical reaction parameter  $L = 0.5, 1.5, 2.5$ , when  $M = 0.01, K_1 = 0.0022$ ,  $Pr = 0.7$ ,  $\beta = 0.1$ ,  $Df = 0.2$ ,  $Ha = 1.5$ ,  $Ec = 0.001$ ,  $Sr = 0.1$ ,  $Sc = 0.2$  and  $K = 2$ .

Fig. (20), the concentration profile is plotted against  $\eta$ , for various values of the Soret number  $Sr = 0.1, 0.5, 0.9$ , when  $M = 0.01, K_1 = 0.0022$ ,  $Pr = 0.7$ ,  $\beta = 0.1$ ,  $Df = 0.2$ ,  $Ha = 1.5$ ,  $Ec = 0.001$ ,  $K = 2$ ,  $Sc = 0.2$  and  $L = 0.5$ .